Cell Reports

Lineage-Restricted Mammary Stem Cells Sustain the Development, Homeostasis, and Regeneration of the Estrogen Receptor Positive Lineage

Graphical Abstract
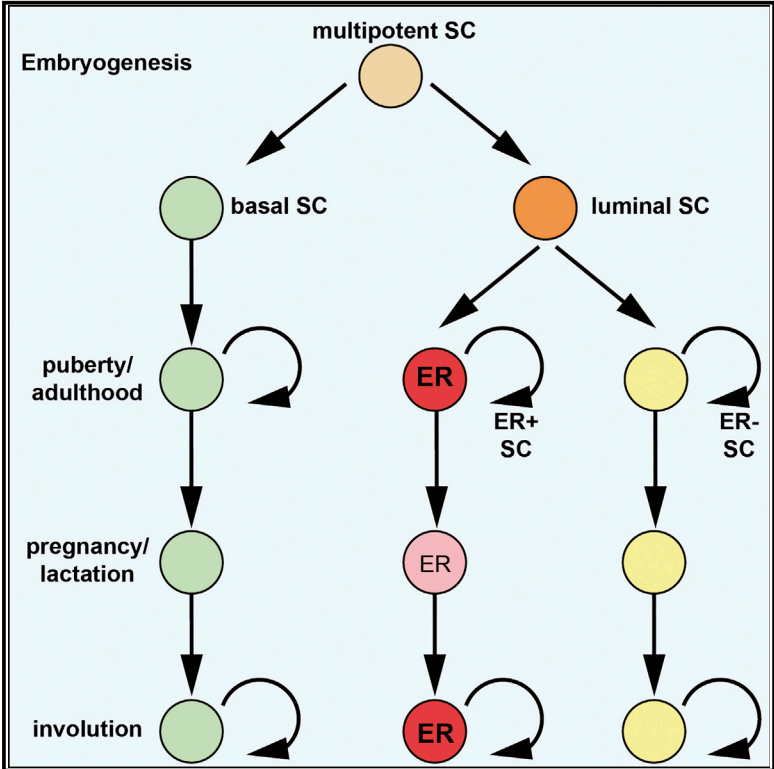
Authors

Alexandra Van Keymeulen,
Marco Fioramonti, Alessia Centonze,
Gaëlle Bouvencourt, Younes Achouri,
Cédric Blanpain

Correspondence

avkeymeu@ulb.ac.be (A.V.K.),
cedric.blanpain@ulb.ac.be (C.B.)

In Brief

Van Keymeulen et al. performed lineage tracing of estrogen receptor (ER)-expressing cells in the mammary gland. They show that the ER^{+} cells are maintained by lineage-restricted stem cells that exclusively contribute to the expansion of the ER[+] lineage during puberty and to their maintenance during adult life.

Highlights

- ER^{+} stem cells mediate expansion and maintenance of the ER[+] lineage

- ER^{+} stem cells expand and differentiate into ER^{+} cells following transplantation

- ER^{+} stem cells survive involution and repopulate the ER[+] lineage

CrossMark

CellPress

Lineage-Restricted Mammary Stem Cells Sustain the Development, Homeostasis, and Regeneration of the Estrogen Receptor Positive Lineage

Alexandra Van Keymeulen,[1,4,*] Marco Fioramonti,[1,4] Alessia Centonze,[1] Gaëlle Bouvencourt,[1] Younes Achouri,[2] and Cédric Blanpain[1,3,5,*]
[1]Laboratory of Stem Cells and Cancer, Université Libre de Bruxelles (ULB), Brussels 1070, Belgium
[2]de Duve Institute, Université Catholique de Louvain, Brussels 1200, Belgium
[3]WELBIO, Université Libre de Bruxelles, Brussels 1070, Belgium
[4]These authors contributed equally
[5]Lead Contact
*Correspondence: avkeymeu@ulb.ac.be (A.V.K.), cedric.blanpain@ulb.ac.be (C.B.)
 http://dx.doi.org/10.1016/j.celrep.2017.07.066

SUMMARY

The mammary gland (MG) is composed of different cell lineages, including the basal and the luminal cells (LCs) that are maintained by distinct stem cell (SC) populations. LCs can be subdivided into estrogen receptor (ER)$^+$ and ER$^-$ cells. LCs act as the cancer cell of origin in different types of mammary tumors. It remains unclear whether the heterogeneity found in luminal-derived mammary tumors arises from a pre-existing heterogeneity within LCs. To investigate LC heterogeneity, we used lineage tracing to assess whether the ER$^+$ lineage is maintained by multipotent SCs or by lineage-restricted SCs. To this end, we generated doxycycline-inducible ER-rtTA mice that allowed us to perform genetic lineage tracing of ER$^+$ LCs and study their fate and long-term maintenance. Our results show that ER$^+$ cells are maintained by lineage-restricted SCs that exclusively contribute to the expansion of the ER$^+$ lineage during puberty and their maintenance during adult life.

INTRODUCTION

The mammary gland (MG) is composed of two main epithelial cell types: the basal cells (BCs), also called myoepithelial cells, and luminal cells (LCs). While LCs secrete water and nutriments to produce the milk during lactation, the BCs, through their contraction, guide the circulation of the milk throughout the ductal tree (Watson and Khaled, 2008). LCs can be subdivided into ductal and alveolar cells and between estrogen (ER)$^+$/progesterone receptor (PR)$^+$ and ER$^-$/PR$^-$ cells (Petersen et al., 1987).

Transplantation of fluorescence-activated cell sorting (FACS)-isolated mammary epithelial cells has shown that a single BC can reconstitute, although at low frequency, a functional MG (Shackleton et al., 2006; Stingl et al., 2006), suggesting that multipotent basal SCs reside at the top of the cellular hierarchy of the MG and give rise to all mammary lineages. While these trans-

plantation experiments are important to define the clonogenic and differentiation potential of SCs, these assays mimic a regenerative state that does not necessarily reflect the natural fate of the cells in physiological conditions (Blanpain and Fuchs, 2014).

It also has been hypothesized that such long-term multipotent basal SCs would give rise to more short-term common luminal progenitors able to differentiate into ER$^+$ and ER$^-$ cells (Visvader and Stingl, 2014). Although LCs expressing ER were, for long time, thought to represent terminally differentiated LCs with low proliferative potential (Russo et al., 1999; Clarke et al., 1997; Seagroves et al., 2000; Ewan et al., 2005), studies have demonstrated that ER$^+$ can be labeled by administration of nucleotide analogs, such as tritiated thymidine or EdU, that are incorporated during DNA synthesis (Zeps et al., 1999; Shyamala et al., 2002; Cheng et al., 2004; Beleut et al., 2010; Giraddi et al., 2015), suggesting that ER$^+$ cells can proliferate. Consistent with this notion, both ER$^+$ and ER$^-$ LCs presenting some clonogenic potential in vitro and in vivo have been isolated by flow cytometry (Welm et al., 2002; Regan et al., 2012; Shehata et al., 2012; Sleeman et al., 2007). Sca1 and CD133 (prominin 1), two cell-surface markers, have been shown to be correlated with ER expression (Sleeman et al., 2007). Within Sca1-expressing LCs, CD49b expression can separate ER$^+$ cells with (Sca1$^+$CD49b$^+$) and without (Sca1$^+$CD49b$^-$) in vitro colony-forming potential and the ability to contribute to MG formation following transplantation in vivo (Shehata et al., 2012). Long-term administration of EdU leads to the labeling of all LC types, which could indicate that each LC population is capable to proliferate but could also reflect a flux of EdU marked cells that transit from one population of LC to another (Giraddi et al., 2015). While these data show that some ER$^+$ and ER$^-$ LCs are capable of proliferation, it remains unclear whether ER$^+$ and ER$^-$ are maintained by a common luminal stem cell (SC) or by distinct types of ER$^+$ and ER$^-$ restricted SCs.

Lineage tracing studies, the gold standard for studying the fate and dynamics of epithelial SCs during physiological conditions (Blanpain and Fuchs, 2014), have been used to decipher the cellular hierarchy in MG development and adult homeostasis. Inducible lineage tracing strategies have allowed us to specifically mark BCs or LCs, and, in doing so, we and others have demonstrated that during puberty and adult life, BCs and LCs expand and are maintained by their own pool of lineage

restricted unipotent SCs (Van Keymeulen et al., 2011; van Amer-ongen et al., 2012; Prater et al., 2014; Lafkas et al., 2013; Rodilla et al., 2015; Scheele et al., 2017; Davis et al., 2016; Blaas et al., 2016; Tao et al., 2014). Transplantation of lineage-restricted BCs labeled by lineage tracing demonstrated the cells' ability to expand their fate in transplantation assays and to give rise to all MG lineages (Van Keymeulen et al., 2011; Prater et al., 2014), showing that transplantation assay might mimic a regen-erative state that stimulates basal SCs to differentiate into luminal lineage. Lineage tracing at saturation, where either all BCs or all LCs are definitively labeled, demonstrated that each and every adult LC is maintained by its own pool of luminal-restricted SCs and is not replaced over time by basal SCs (Wui-dart et al., 2016). It is still unclear, however, whether the luminal lineage is composed of heterogeneous populations of luminal stem and progenitor cells.

Lineage tracing using the Wap-cre, which is active in luminal alveolar ER⁻ cells during pregnancy only, demonstrated that Wap-labeled ER⁻ LCs during a first pregnancy give rise to ER⁻ LCs during a second pregnancy (Chang et al., 2014), suggesting that ER⁻ lineage can be sustained by a separate pool of SCs compared to the ER⁺ lineage. Consistent with this notion, more recent lineage tracing experiments showed that Notch1-labeled and Sox9-labeled ER⁻ luminal populations, which have long-term self-renewing potential, give rise to ductal and alveolar ER⁻ cells only, further demonstrating that a fraction of ER⁻ LCs are maintained by a distinct pool of SCs (Rodilla et al., 2015; Wang et al., 2017). However, these data do not allow us to define the origin of ER⁺ cells or determine whether ER⁺ cells share a common precursor with other ER⁻ LCs that would not have been targeted by the Notch1CREER or the Sox9CREER. Prominin1CREER, which targets a fraction of ER⁺ LCs, showed that ER⁺ cells gave rise to ER⁺ cells only. However, as Prominin1CREER only labeled 2% of Sca1⁺ LCs, it remains un-clear if Prominin1CREER-labeled cells are representative of the whole ER⁺ LC population (Wang et al., 2017).

Different studies have demonstrated that LCs are the cancer cell of origin of different mammary tumors. Targeting LCs with Brca1/p53 deletion or oncogenic pik3ca demonstrated that LCs are more potent at inducing tumor formation than are BCs and that tumors arising from LCs are usually more aggressive and more heterogeneous (Molyneux et al., 2010; Blaas et al., 2016; Van Keymeulen et al., 2015; Koren et al., 2015). It remains unclear from these studies whether the heterogeneity of luminal-derived tumors arises from the initial targeting of heterogeneous populations of luminal stem and progenitor cells or whether LCs are more plastic during oncogenic transformation.

To investigate LC heterogeneity and identify the origin of ER⁺ LCs and the mechanisms regulating their pubertal expansion and adult maintenance, we generated a transgenic ER-rtTA mouse, in which the TetOn tetracycline transactivator is ex-pressed under the control of the *esr1* promoter, allowing us to perform doxycycline (Dox)-inducible lineage tracing of ER⁺ LCs and assessing their fate over time. We found that the ER⁺ lineage is maintained by lineage-restricted ER⁺ luminal SCs that ensure ER⁺ lineage expansion during pubertal development and the long-term renewing capacities of ER⁺ lineage in adult mice during cycles of pregnancy, lactation, and involution.

RESULTS

ER Expression during MG Development and Homeostasis

Immunostaining for ER during mouse MG development and adult life showed that during embryonic development, ER was not expressed in the MG epithelium and its expression was restricted to the mammary mesenchyme. ER became highly ex-pressed in the MG epithelium around postnatal day 7 (P7) in a fraction of LCs (50%). The proportion of LCs expressing ER (around 50%) remained constant during the pubertal expansion and in adult virgin mice. Upon pregnancy, the proportion of ER LCs dramatically decreased, only 5% of LCs expressed ER at the end of the pregnancy, and no ER⁺ cells were observed dur-ing lactation (Figures 1A and 1B). After MG involution that accompanied the end of lactation, the proportion of ER⁺ re-turned to their initial value found in adult virgin mice (Figures 1A and 1B). These data show that the ER is dynamically expressed during MG development and adult life. Whether this dynamic expression of ER is the result of a regulated expression of ER in equipotent luminal SCs at different stages of MG development and adult remodeling or through a different clonal dynamic of ER⁺ and ER⁻ restricted SCs during these different stages remains unclear.

To assess whether LC heterogeneity is associated with differ-ential proliferation within the MG epithelium, we assessed the proliferation rate of ER⁺ and ER⁻ LCs. To this end, we quantified by FACS bromodeoxyuridine (BrdU) incorporation in Sca1⁺ and Sca1⁻ CD24⁺CD29^Lo cells that represent ER⁺ and ER⁻ LCs (Sleeman et al., 2007; Shehata et al., 2012). We found that Sca1⁻ CD24⁺CD29^Lo cells presented a higher rate of prolifera-tion, both during pubertal MG expansion and in adulthood, although 8% and 2% of Sca1⁺ incorporated BrdU in puberty and in adulthood, respectively (Figure 1C). These data are consistent with previously published studies using other methods to assess proliferation in the MG (Shyamala et al., 2002; Giraddi et al., 2015) and show that a fraction of ER⁺ LCs are actively proliferating during pubertal expansion and in adult virgin mice.

Generation of Genetically Engineered Dox-Inducible ER-rtTA Mice

To determine whether all ER⁺ LCs are maintained by lineage-restricted ER⁺ SCs or whether some ER⁺ LCs are maintained by ER⁻ LCs or other cells, we generated a genetically engineered mouse model that allowed us to specifically target ER⁺ cells. To avoid using tamoxifen, which can induce delay of MG develop-ment (Shehata et al., 2014; Van Keymeulen et al., 2015), we generated ER-rtTA transgenic mice that allowed us to target ER-expressing cells following Dox administration and to perform lineage tracing studies. The 4-kb fragment upstream of the *Esr1* transcription starting site was cloned into a vector containing rtTA and was injected into fertilized oocytes. We identified four positive founders by PCR. We bred the ER-rtTA founder mice with TetO-H2B-GFP mice (Tumbar et al., 2004) and found that one founder faithfully expressed H2B-GFP in ER⁺ LCs of the MG (Figures 2A and 2B). This founder mouse was used throughout this study.
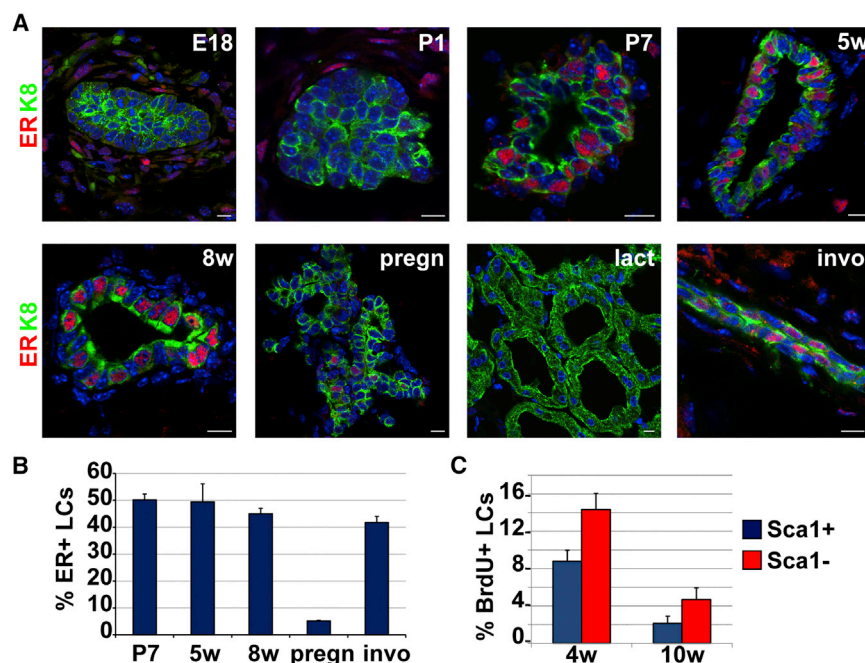
Figure 1. ER Expression and Luminal Cell Proliferation during MG Development and Adulthood

(A) Immunostaining of ER (red), K8 (green), and nuclei (blue) in wild-type MG at E18, birth (P1), 7 days old (P7), puberty (5w), adulthood (8w), 14 days pregnancy (pregn), during lactation (lact), and after involution (invo).

(B) Quantification of ER expression in K8+ luminal cells at different MG developmental stages.

(C) FACS quantification of BrdU incorporation in Sca1+ and Sca1− CD29Lo/CD24+ LCs in 4- and 10-week-old mice. Histograms and error bars represent the mean and SEM.

See the Supplemental Experimental Procedures for more details on quantification. Scale bars, 10 μm.

As we marked 50% of ER+ LCs in these experiments, we could not exclude that a fraction of unlabeled cells are replaced by another source of cells rather than by lineage-restricted ER+ SCs. To distinguish between these possibilities, we performed lineage tracing at saturation to label all ER+ LCs. To this end, we administered Dox during the whole period of MG pubertal expansion and assessed the cells' fate during adulthood (Figure 2K). One month of continuous Dox administration lead to the labeling of all ER+ LCs during puberty (Figure 2L). After a month of chase, all ER+ LCs were still YFP+ (Figures 2M and 2N), demonstrating that all ER+ LCs are self-maintained by ER+ SCs and not replaced by another cell type.

Upon Dox administration in ER-rtTA/TetOCRE/Rosa-YFP mice, labeled LCs (YFP+ CD24+CD29Lo) were all Sca1+ and CD133+ and were either CD49b+ or CD49b−, but no Sca1− CD49b+ cells were labeled (Figures 2O–2S and S2), consistent with previous report showing that Sca1 and CD133 mark ER+ LCs (Sleeman et al., 2007; Shehata et al., 2012). The proportion of labeled cells in these cell populations (YFP+ CD24+CD29Lo Sca1+ CD49b+ and YFP+ CD24+CD29Lo Sca1+ CD49b−) remained constant during pubertal expansion and adult remodeling, showing that ER+ LCs are sustained by their own pool of lineage-restricted SCs that are not replaced over time by other unlabeled populations.

ER+ LCs Maintain ER Lineage during Cycles of Pregnancy, Lactation, and Involution

During pregnancy, the proportion of ER+ cells drops dramatically, due to the expansion of ER− expressing cells that differentiate into alveolar milk-producing cells (Rodilla et al., 2015). However, at the end of the involution stage, the proportion of ER+ expressing cells is similar to the pre-pregnancy level (Figures 1A and 1B). It is still unclear whether ER+ cells selectively survive from involution or whether ER expression is dynamically regulated in LCs and is expressed by ER− cells after involution.

To address this question, we labeled ER+ cells during puberty by Dox administration to ER-rtTA/TetOCRE/Rosa-YFP mice and

ER+ Luminal SCs Mediated the Expansion of the ER Lineage during Pubertal Development

To assess the fate of ER+ LCs and the mechanisms that ensure their development and long-term maintenance, we performed Dox-inducible ER lineage tracing experiments by crossing ER-rtTA mice with TetOCRE/Rosa-YFP reporter mice (Perl et al., 2002; Srinivas et al., 2001). We first assessed whether the ER+ cell expansion occurring during puberty is mediated by equipotent and multipotent luminal SCs or by lineage-restricted ER+ SCs by administering Dox to ER-rtTA/TetOCRE/Rosa-YFP mice for 5 days starting at P28. In the absence of Dox administration or ER-rtTA transgene, a small leakiness was observed in mesenchymal cells but no mammary epithelial cells were labeled, demonstrating the absence of leakiness of the ER-rtTA in the mammary epithelium (Figures 2E and S1). After 5 days of Dox administration, only LCs expressing ER were initially labeled, and 99.5% of YFP+ LCs expressed high levels of ER as examined by immunostaining (Figure 2F), demonstrating the high specificity of ER targeting using the ER-rtTA/TetOCRE/Rosa-YFP mice. About 20% of LCs were YFP labeled as soon as 3 days following Dox administration, which corresponds to about 50% of the ER+ LCs (Figure 2G). Interestingly, the proportion of LCs that were YFP labeled at the end of the pubertal development (4 week chase) and during adult remodeling (10-week chase) did not change significantly (Figure 2G), despite the 4-fold expansion of the luminal population (Figure 2H) and similar ratio of ER+ cells at these two time points (Figure 1B), showing that the expansion of the ER+ lineage is not mediated by a population of unlabeled ER- LCs or basal cells but is rather mediated by ER+ SCs. These labeled LCs were all ER+ (Figures 2I and 2J), showing that ER+ SCs only give rise to ER+ LC lineage.

Figure 2. ER⁺ Luminal SCs Ensure Expansion and Maintenance of the ER⁺ Luminal Lineage during Pubertal Development and Adult Mice

(A) Genetic strategy to functionally test ER-rtTA founders.

(B) Immunostaining of ER (red), GFP (green), and nuclei (blue) in MG of adult ER-rtTA/TetOH2B-GFP mice following 5 days doxycycline (Dox) administration showing H2B-GFP expression only in ER⁺ LCs.

(C and D) Genetic (C) and experimental (D) strategies to lineage trace ER⁺ LCs and analyze their fate over time.

(E and F) Immunostaining of ER (red), YFP (green), K14 (white), and nuclei (blue) in MG from 5-week-old ER-rtTA/TetOCre/RosaYFP mice without Dox (E) and following 5 days Dox food (F), showing expression of YFP in ER⁺ LCs following DOX induction.

(G) Percentage of YFP⁺ cells in luminal population defined by $CD24^+CD29^{Lo}$ expression at different time points in MG from ER-rtTA/TetOCre/RosaYFP mice induced at 4 weeks old, showing that the proportion of labeled cells remained constant over time.

(H) Absolute number of $CD24^+CD29^{Lo}$ cells during pubertal expansion as quantified by FACS.

(I and J) Immunostaining of ER (red), YFP (green), and nuclei (blue) in MG from ER-rtTA/TetOCre/RosaYFP mice induced at 4 weeks old and analyzed 4 (I) and 10 weeks (J) later.

(K) Experimental strategy of the lineage tracing at saturation.

(L and M) Immunostaining of ER (red), YFP (green), and nuclei (blue) in MG from ER-rtTA/TetOCre/RosaYFP mice induced at saturation at the end of Dox treatment (sat-0) (L) and 4 weeks later (sat-4w) (M).

(N) Quantification of YFP⁺ cells in ER⁺ K8⁺ LCs in saturation experiments (four mice were analyzed for each time point).

(O–S) FACS analysis of Sca1 and CD49b (O and P) or CD133 and CD49b (Q and R) in total $CD24^+CD29^{Lo}$ LCs (O and Q) or in YFP⁺ $CD24^+CD29^{Lo}$ LCs (P, R, and S), showing that ER-derived YFP⁺ LCs are Sca1⁺ and CD133⁺.

See the Supplemental Experimental Procedures for more details on quantifications. Histograms and error bars represent the mean and SEM. Scale bars, 10 μm. See also Figures S1 and S2.

mated them when 8 weeks old. We analyzed the mice when they were 2 weeks' pregnant, lactating since 2 weeks, 6 weeks after weaning, and after a complete second cycle of pregnancy, lactation, and involution (Figure 3A). After 2 weeks of pregnancy, the proportion of YFP⁺ cells dramatically decreased proportionally to the decrease of ER⁺ cells observed by immunostaining, and labeled cells were observed both in ductal and in alveolar regions (Figures 3B–3E). During lactation, rare YFP⁺ cells were scattered in the alveoli, but did not show detectable ER expression (Figures 3F and 3G). All YFP-labeled cells were PR⁺, showing ER-derived cells maintain their hormone responsive potential, albeit not

currently expressing ER (Figure 3H). After involution, YFP⁺ cells were observed at a frequency similar to the one observed before pregnancy, and all YFP⁺ cells expressed ER, showing the labeled ER⁺ cells kept their ER⁺ identity through the cycle of pregnancy, lactation, and involution and that ER⁺ cells do not arise from ER⁻ cells after involution (Figure 3I).

FACS analysis of the proportion of YFP⁺ LCs at different stages showed that although the proportion of YFP⁺ cells dramatically decreased during pregnancy, it returned to the proportion observed before pregnancy after involution following one or two cycles of pregnancy, lactation, and involution (Figure 3J).
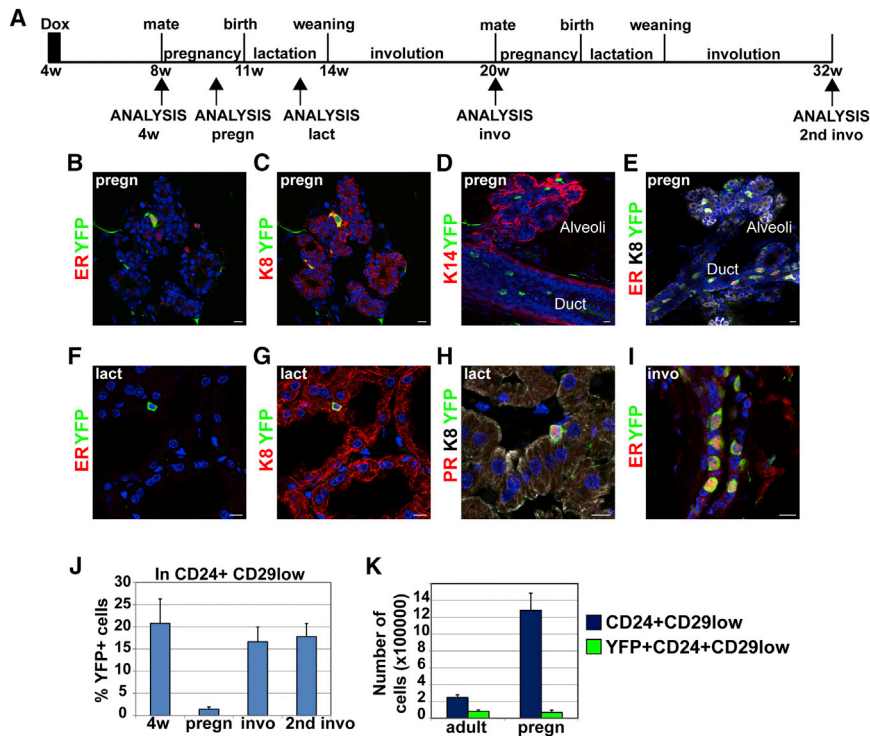
Figure 3. ER+ Luminal SCs Ensure Maintenance of ER+ Lineage during Cycles of Pregnancy, Lactation, and Involution

(A) Experimental strategy to induce lineage tracing of ER+ LCs at the onset of puberty and analyze their fate at different time points during cycle of pregnancy, lactation, and involution.

(B–E) Immunostaining of YFP and ER (B and E), K8 (C and E), K14 (D), and nuclei in MG from ER-rtTA/TetOCre/RosaYFP mice induced at 4 weeks old during pregnancy showing scarce ductal and alveoli YFP+ ER+ cells during pregnancy.

(F–H) Immunostaining in the MG from ER-rtTA/TetOCre/RosaYFP mice induced at 4 weeks old during lactation, showing scarce YFP+ ER− (F), K8+ (G), and PR+ (H) cells in alveoli.

(I) Immunostaining of ER (red) and YFP (green) in MG from ER-rtTA/TetOCre/RosaYFP mice induced at 4 weeks and analyzed after involution.

(J) Percentage of YFP+ cells in CD24+CD29Lo expression at different time points, showing that the proportion of ER+-labeled LCs decreases during the pregnancy, but returns to levels similar to those before pregnancy after involution.

(K) Absolute number of LCs and ER-derived YFP+ LCs based on CD24+CD29Lo expression during pregnancy, showing that the total LCs expand by 5-fold, whereas ER-derived YFP+ LCs remain constant.

See the Supplemental Experimental Procedures for more details on quantifications. Histograms and error bars represent mean and SEM. Scale bars, 10 μm.

Quantification of the absolute number of LCs before and during pregnancy showed that the number of YFP+ ER-derived cells remained constant (Figure 3K), although their relative proportion decreased during pregnancy due to the expansion of the ER− cells. These results demonstrate that ER+ and ER− cells represent distinct self-sustained lineages during cycles of pregnancy, lactation, and involution.

ER+ Adult LCs Have Regenerative Potential following Transplantation

Transplantation assays have been used for decades to assess SC potential in the MG (Deome et al., 1959; Visvader and Stingl, 2014). Whereas BCs are multipotent when transplanted alone, when BCs and LCs are transplanted together they maintain their lineage-restricted fate, similarly to physiological conditions (Van Keymeulen et al., 2011). To assess whether ER+ derived LCs are able to expand and contribute to repopulating activity of the ER lineage in transplantation assays, MGs from 10-week-old ER-rtTA/TetOCRE/Rosa-YFP treated with Dox to induce YFP expression in ER+ LCs were harvested, dissociated into small fragments or single cells, and grafted into immunodeficient mice (Figures 4A and 4F). Out of 13 grafts, we observed 12 YFP+ outgrowths and 1 YFP− outgrowth in MG fragment, and out of 15 grafts, we observed 14 YFP+ and 1 YFP− outgrowth in single-cell transplantation. In each YFP+ outgrowth, YFP+ ER-derived cells contributed to the repopulation of ER+ lineage and did not contribute to other lineages (Figures 4B–4J). These results clearly demonstrate the regenerative and lineage-restricted potential of adult ER+ luminal SCs.

DISCUSSION

Our ER lineage tracing experiments provide clear evidence that the ER+ lineage is maintained by a distinct pool of lineage-restricted luminal SCs independent of the ER− luminal lineage. Our data show that ER+ luminal lineage expands and is maintained by ER+ luminal SCs, and not by ER− luminal SCs. Lineage tracing at saturation, where all ER+ cells are labeled, shows that ER+ SCs exclusively contribute to the ER+ lineage, and not at all to the ER− lineage. Moreover, our data also demonstrate that, once specified, ER+ luminal cells are exclusively maintained by ER+ SCs, and not by a common progenitor for ER+ and ER− lineages under physiological conditions, including puberty MG expansion, adulthood, and cycles of pregnancy, lactation, and involution. Transplantation experiments further demonstrate the high regenerative potential of ER+ luminal SCs. Our data allow to substantially revise the current model of the cellular hierarchy that maintains MG and provide clear evidences that the ER+ and ER− cells are maintained by distinct pools of lineage-restricted luminal SCs, consistent with other recent studies (Rodilla et al., 2015; Wang et al., 2017).

Our ER-rtTA mice and ER lineage tracing approaches will be instrumental in isolating with high purity ER+ cells at different stages of MG development and adult remodeling. These mice also will be used to specifically ablate the ER+ LC lineage and assess the cells' essential and non-redundant role in mediating MG development and cycles of pregnancy, lactation, and involution. Finally, these mice will be used to assess whether tumor
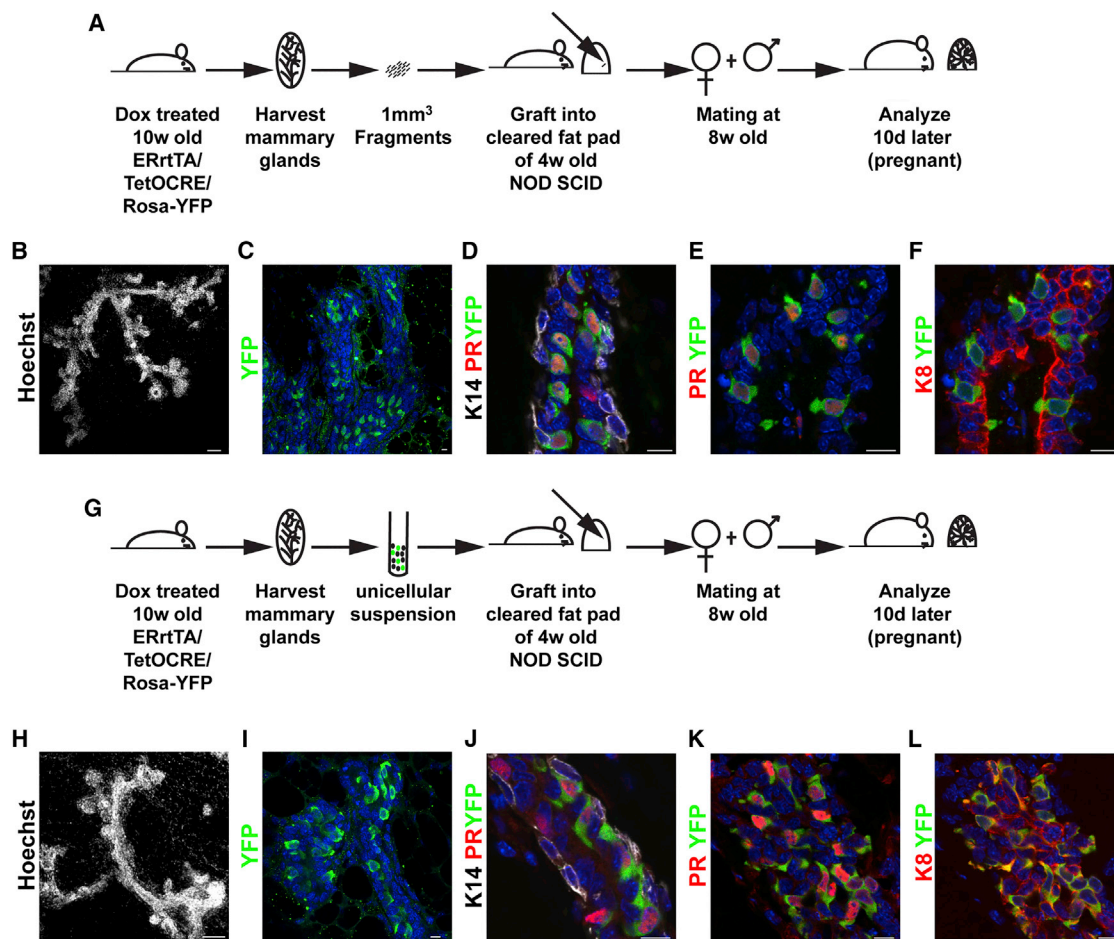
Figure 4. ER$^+$ Adult LCs Have Renewal and Lineage-Restricted Potential following Transplantation

(A) Experimental strategy to transplant MG fragments of 10-week-old ER-rtTA/TetOCre/RosaYFP mice induced 5 days with Dox at 4 weeks old.

(B–F) Immunofluorescence of Hoechst (B), YFP (C–F), and PR (D and E), K14 (D), or K8 (F) in MG outgrowth following MG fragment transplantation, showing that YFP$^+$ were all PR$^+$.

(G) Experimental strategy to transplant 100,000 cells containing ER$^+$ YFP$^+$-labeled LCs, unlabeled ER- LCs, and BCs of 10-week-old ER-rtTA/TetOCre/RosaYFP mice induced 5 days with Dox at 4 weeks old.

(H–L) Immunofluorescence of Hoechst (H), YFP (I–L), and PR (J and K), K14 (J), or K8 (L) in MG outgrowth following transplantation of unsorted cells from ER-rtTA/TetOCre/RosaYFP mice, showing YFP$^+$ LCs were all PR$^+$.

Scale bars in (C)–(F) and (I)–(L) represent 10 μm. Scale bars in (B) and (H) represent 100 μm.

heterogeneity found in luminal-derived mammary tumors is the consequence of pre-existing of luminal cell heterogeneity between the ER$^+$ and ER$^-$ cells or through their high plasticity of LCs following oncogenic transformation.

EXPERIMENTAL PROCEDURES

ER-rtTA Mice Generation

ER-rtTA transgenic mice were generated using the 4-kb sequence upstream of the ATG codon of the murine Esr1 gene, β-globin intron, the rtTA fragment from the pTetON Advanced plasmid and the SV40 polyA signal. Detailed procedures are described in the Supplemental Experimental Procedures.

Immunostaining, Mammary Cell Flow Cytometry, and Quantifications

Detailed protocols for immunostaining, mammary cell flow cytometry, and quantifications are described in the Supplemental Experimental Procedures.

Cleared Mammary Fat Pad Transplantation

1 mm^3 fragments or 100,000 unsorted cells in unicellular suspension generated from Dox-treated adult ER-rtTA/TetOCRE/RosaYFP mice were transplanted into cleared fat pad from 4-week-old Nod Scid mice. Detailed procedures are described in the Supplemental Experimental Procedures.

SUPPLEMENTAL INFORMATION

Supplemental Information includes Supplemental Experimental Procedures and two figures and can be found with this article online at http://dx.doi.org/10.1016/j.celrep.2017.07.066.

AUTHOR CONTRIBUTIONS

REFERENCES

Beleut, M., Rajaram, R.D., Caikovski, M., Ayyanan, A., Germano, D., Choi, Y., Schneider, P., and Brisken, C. (2010). Two distinct mechanisms underlie progesterone-induced proliferation in the mammary gland. Proc. Natl. Acad. Sci. USA 107, 2989–2994.

Blaas, L., Pucci, F., Messal, H.A., Andersson, A.B., Josue Ruiz, E., Gerling, M., Douagi, I., Spencer-Dene, B., Musch, A., Mitter, R., et al. (2016). Lgr6 labels a rare population of mammary gland progenitor cells that are able to originate luminal mammary tumours. Nat. Cell Biol. 18, 1346–1356.

Blanpain, C., and Fuchs, E. (2014). Stem cell plasticity. Plasticity of epithelial stem cells in tissue regeneration. Science 344, 1242281.

Chang, T.H., Kunasegaran, K., Tarulli, G.A., De Silva, D., Voorhoeve, P.M., and Pietersen, A.M. (2014). New insights into lineage restriction of mammary gland epithelium using parity-identified mammary epithelial cells. Breast Cancer Res. 16, R1.

Cheng, G., Weihua, Z., Warner, M., and Gustafsson, J.A. (2004). Estrogen receptors ER alpha and ER beta in proliferation in the rodent mammary gland. Proc. Natl. Acad. Sci. USA 101, 3739–3746.

Clarke, R.B., Howell, A., Potten, C.S., and Anderson, E. (1997). Dissociation between steroid receptor expression and cell proliferation in the human breast. Cancer Res. 57, 4987–4991.

Davis, F.M., Lloyd-Lewis, B., Harris, O.B., Kozar, S., Winton, D.J., Muresan, L., and Watson, C.J. (2016). Single-cell lineage tracing in the mammary gland reveals stochastic clonal dispersion of stem/progenitor cell progeny. Nat. Commun. 7, 13053.

Deome, K.B., Faulkin, L.J., Jr., Bern, H.A., and Blair, P.B. (1959). Development of mammary tumors from hyperplastic alveolar nodules transplanted into gland-free mammary fat pads of female C3H mice. Cancer Res. 19, 515–520.

Ewan, K.B., Oketch-Rabah, H.A., Ravani, S.A., Shyamala, G., Moses, H.L., and Barcellos-Hoff, M.H. (2005). Proliferation of estrogen receptor-alpha-positive mammary epithelial cells is restrained by transforming growth factor-beta1 in adult mice. Am. J. Pathol. 167, 409–417.

Giraddi, R.R., Shehata, M., Gallardo, M., Blasco, M.A., Simons, B.D., and Stingl, J. (2015). Stem and progenitor cell division kinetics during postnatal mouse mammary gland development. Nat. Commun. 6, 8487.

Koren, S., Reavie, L., Couto, J.P., De Silva, D., Stadler, M.B., Roloff, T., Britschgi, A., Eichlisberger, T., Kohler, H., Aina, O., et al. (2015). PIK3-CA(H1047R) induces multipotency and multi-lineage mammary tumours. Nature 525, 114–118.

Lafkas, D., Rodilla, V., Huyghe, M., Mourao, L., Kiaris, H., and Fre, S. (2013). Notch3 marks clonogenic mammary luminal progenitor cells in vivo. J. Cell Biol. 203, 47–56.

Molyneux, G., Geyer, F.C., Magnay, F.A., McCarthy, A., Kendrick, H., Natrajan, R., Mackay, A., Grigoriadis, A., Tutt, A., Ashworth, A., et al. (2010). BRCA1 basal-like breast cancers originate from luminal epithelial progenitors and not from basal stem cells. Cell Stem Cell 7, 403–417.

Perl, A.K., Wert, S.E., Nagy, A., Lobe, C.G., and Whitsett, J.A. (2002). Early restriction of peripheral and proximal cell lineages during formation of the lung. Proc. Natl. Acad. Sci. USA 99, 10482–10487.

Petersen, O.W., Høyer, P.E., and van Deurs, B. (1987). Frequency and distribution of estrogen receptor-positive cells in normal, nonlactating human breast tissue. Cancer Res. 47, 5748–5751.

Prater, M.D., Petit, V., Alasdair Russell, I., Giraddi, R.R., Shehata, M., Menon, S., Schulte, R., Kalajzic, I., Rath, N., Olson, M.F., et al. (2014). Mammary stem cells have myoepithelial cell properties. Nat. Cell Biol. 16, 942–950, 1–7.

Regan, J.L., Kendrick, H., Magnay, F.A., Vafaizadeh, V., Groner, B., and Smalley, M.J. (2012). c-Kit is required for growth and survival of the cells of origin of Brca1-mutation-associated breast cancer. Oncogene 31, 869–883.

Rodilla, V., Dasti, A., Huyghe, M., Lafkas, D., Laurent, C., Reyal, F., and Fre, S. (2015). Luminal progenitors restrict their lineage potential during mammary gland development. PLoS Biol. 13, e1002069.

Russo, J., Ao, X., Grill, C., and Russo, I.H. (1999). Pattern of distribution of cells positive for estrogen receptor alpha and progesterone receptor in relation to proliferating cells in the mammary gland. Breast Cancer Res. Treat. 53, 217–227.

Scheele, C.L., Hannezo, E., Muraro, M.J., Zomer, A., Langedijk, N.S., van Oudenaarden, A., Simons, B.D., and van Rheenen, J. (2017). Identity and dynamics of mammary stem cells during branching morphogenesis. Nature 542, 313–317.

Seagroves, T.N., Lydon, J.P., Hovey, R.C., Vonderhaar, B.K., and Rosen, J.M. (2000). C/EBPbeta (CCAAT/enhancer binding protein) controls cell fate determination during mammary gland development. Mol. Endocrinol. 14, 359–368.

Shackleton, M., Vaillant, F., Simpson, K.J., Stingl, J., Smyth, G.K., Asselin-Labat, M.L., Wu, L., Lindeman, G.J., and Visvader, J.E. (2006). Generation of a functional mammary gland from a single stem cell. Nature 439, 84–88.

Shehata, M., Teschendorff, A., Sharp, G., Novcic, N., Russell, I.A., Avril, S., Prater, M., Eirew, P., Caldas, C., Watson, C.J., and Stingl, J. (2012). Phenotypic and functional characterisation of the luminal cell hierarchy of the mammary gland. Breast Cancer Res. 14, R134.

Shehata, M., van Amerongen, R., Zeeman, A.L., Giraddi, R.R., and Stingl, J. (2014). The influence of tamoxifen on normal mouse mammary gland homeostasis. Breast Cancer Res. 16, 411.

Shyamala, G., Chou, Y.C., Louie, S.G., Guzman, R.C., Smith, G.H., and Nandi, S. (2002). Cellular expression of estrogen and progesterone receptors in mammary glands: regulation by hormones, development and aging. J. Steroid Biochem. Mol. Biol. 80, 137–148.

Sleeman, K.E., Kendrick, H., Robertson, D., Isacke, C.M., Ashworth, A., and Smalley, M.J. (2007). Dissociation of estrogen receptor expression and in vivo stem cell activity in the mammary gland. J. Cell Biol. 176, 19–26.

Srinivas, S., Watanabe, T., Lin, C.S., William, C.M., Tanabe, Y., Jessell, T.M., and Costantini, F. (2001). Cre reporter strains produced by targeted insertion of EYFP and ECFP into the ROSA26 locus. BMC Dev. Biol. 1, 4.

Stingl, J., Eirew, P., Ricketson, I., Shackleton, M., Vaillant, F., Choi, D., Li, H.I., and Eaves, C.J. (2006). Purification and unique properties of mammary epithelial stem cells. Nature 439, 993–997.

Tao, L., van Bragt, M.P., Laudadio, E., and Li, Z. (2014). Lineage tracing of mammary epithelial cells using cell-type-specific cre-expressing adenoviruses. Stem Cell Reports 2, 770–779.

Tumbar, T., Guasch, G., Greco, V., Blanpain, C., Lowry, W.E., Rendl, M., and Fuchs, E. (2004). Defining the epithelial stem cell niche in skin. Science 303, 359–363.

van Amerongen, R., Bowman, A.N., and Nusse, R. (2012). Developmental stage and time dictate the fate of Wnt/β-catenin-responsive stem cells in the mammary gland. Cell Stem Cell 11, 387–400.

Van Keymeulen, A., Rocha, A.S., Ousset, M., Beck, B., Bouvencourt, G., Rock, J., Sharma, N., Dekoninck, S., and Blanpain, C. (2011). Distinct stem cells contribute to mammary gland development and maintenance. Nature *479*, 189–193.

Van Keymeulen, A., Lee, M.Y., Ousset, M., Brohée, S., Rorive, S., Giraddi, R.R., Wuidart, A., Bouvencourt, G., Dubois, C., Salmon, I., et al. (2015). Reactivation of multipotency by oncogenic PIK3CA induces breast tumour heterogeneity. Nature *525*, 119–123.

Visvader, J.E., and Stingl, J. (2014). Mammary stem cells and the differentiation hierarchy: current status and perspectives. Genes Dev. *28*, 1143–1158.

Wang, C., Christin, J.R., Oktay, M.H., and Guo, W. (2017). Lineage-biased stem cells maintain estrogen-receptor-positive and -negative mouse mammary luminal lineages. Cell Rep. *18*, 2825–2835.

Watson, C.J., and Khaled, W.T. (2008). Mammary development in the embryo and adult: a journey of morphogenesis and commitment. Development *135*, 995–1003.

Welm, B.E., Tepera, S.B., Venezia, T., Graubert, T.A., Rosen, J.M., and Goodell, M.A. (2002). Sca-1(pos) cells in the mouse mammary gland represent an enriched progenitor cell population. Dev. Biol. *245*, 42–56.

Wuidart, A., Ousset, M., Rulands, S., Simons, B.D., Van Keymeulen, A., and Blanpain, C. (2016). Quantitative lineage tracing strategies to resolve multipotency in tissue-specific stem cells. Genes Dev. *30*, 1261–1277.

Zeps, N., Bentel, J.M., Papadimitriou, J.M., and Dawkins, H.J. (1999). Murine progesterone receptor expression in proliferating mammary epithelial cells during normal pubertal development and adult estrous cycle. Association with eralpha and erbeta status. J. Histochem. Cytochem. *47*, 1323–1330.

Supplemental Information

Lineage-Restricted Mammary Stem Cells Sustain

the Development, Homeostasis, and Regeneration

of the Estrogen Receptor Positive Lineage

Alexandra Van Keymeulen, Marco Fioramonti, Alessia Centonze, Gaëlle Bouvencourt, Younes Achouri, and Cédric Blanpain

Supplemental Experimental Procedures

Mice. RosaYFP (Srinivas et al., 2001) mice were obtained from the Jackson Laboratory. TetOCre (Perl et al., 2002) mice were provided by A. Nagy. TetOH2B-GFP (Tumbar et al., 2004) mice were provided by E. Fuchs. Mice colonies were maintained in a certified animal facility in accordance with European guidelines. These experiments were approved by the local ethical committee (CEBEA).

Generation of ER-rtTA mice. The rtTA fragment from pTetON Advanced plasmid preceded by the β-globin intron and followed by a SV40 polyA signal was subcloned into pBluescript II SK+. The 4-kb sequence upstream the ATG codon of the murine Esr1 gene, obtained from the BAC clone RP24-222G13 (BACPAC Resources Center, Children's Hospital Oakland Research Institute) using the forward primer 5'-ATGTTGGCTTATGGTTTGAATGGG-3' and the reverse primer 5'-TGCAGAGACTCAGAAGCAAAGAGC-3', was cloned upstream of the β-globin intron. The resulting ER-rtTA fragment of 5.6 kb was released from the backbone by NotI digestion and was microinjected into fertilized oocytes to generate transgenic mice (in the transgenic facility of the Université catholique de Louvain, Brussels, Belgium). 4 transgenic founders were first identified by PCR, out of 34 mice born. Expression profiles of the ER-rtTA founders were screened with reporter TetOH2B-GFP mice. 1 founder expressed the GFP in cells expressing the endogenous ER, and was used throughout this study.

Targeting H2B-GFP expression. ER-rtTA/TetOH2B-GFP adult female mice were induced by oral administration of doxycycline food diet (1g/kg, BIO-SERV) during 5 days and analyzed at the end of the treatment.

Targeting YFP expression. 4 weeks old ER-rtTA/TetOCre/RosaYFP female mice were induced by oral administration of doxycycline food diet (1g/kg, BIO-SERV)

during 5 days, and analyzed at different time points after induction, as specified in figure legends. For saturation experiments, 4 weeks old ER-rtTA/TetOCre/RosaYFP female mice were induced by oral administration of doxycycline food diet (1g/kg, BIO-SERV) combined with doxycycline diluted in drinking water (2g/l, AG Scientific) and 3 intraperitoneal injections per week (200µl of 10mg/ml doxycycline diluted in PBS) during 28 days.

Histology and immunostaining. Dissected MGs were pre-fixed for 2h in 4% paraformaldehyde at room temperature. Tissues were washed three times with PBS for 5 min and incubated overnight in 30% sucrose in PBS at 4°C. Tissues were embedded in OCT compound (Tissue Tek) and kept at -80°C. 5 µm sections were cut using a HM560 Microm cryostat (Mikron Instrument).

Sections were incubated in blocking buffer (5% horse serum/ 1% bovine serum albumin/ 0,2% Triton in PBS) for 1h at room temperature. Primary antibodies were incubated overnight at 4°C. Sections were rinsed three times for 5 min in PBS and incubated with secondary antibodies in blocking buffer for 1 hour at room temperature. Nuclei were stained With Hoechst 33342 dye (Sigma) and slides were mounted in mounting medium (DAKO) supplemented with 2,5% Dabco (Sigma).

For figures 3D, 3E, 4B and 4G, thick sections of 100 µm were cut and staining was performed as for the 5 µm sections, except that the secondary antibodies were incubated overnight at 4°C instead of 1 hour at room temperature.

The following primary antibodies were used: Anti-ERα (Rabbit, 1/500, sc-542, Santa Cruz Biotechnology), Anti-K8 TROMA-1 (Rat, 1/1000, Developmental Studies Hybridoma Bank), Anti K14 (Chicken, 1/1000, PRB-155P-0100, Covance), Anti-GFP (Chicken 1/2000, ab13970, Abcam), Anti-GFP (Goat 1/1000, ab6673, Abcam), Anti-PR (Rabbit 1/200, MA5-14505, ThermoFisher Scientific).

The following secondary antibodies were used: Anti-Rat RRX-conjugated (1/400, Jackson), Anti-Rat Cy5-conjugated (1/400, Jackson), Anti-Rat AlexaFluor 488-conjugated (1/400, LifeTechnology), Anti-Rabbit RRX-conjugated (1/400, Jackson), Anti-Rabbit AlexaFluor 488-conjugated (1/400, LifeTechnology), Anti-Chicken Cy5-conjugated (1/400, Jackson), Anti-Chicken AlexaFluor 488-conjugated (1/400, LifeTechnology), Anti-Goat AlexaFluor 488-conjugated (1/400, LifeTechnology).

Microscope image acquisition. Unless otherwise stated, images were acquired at room temperature using a Zeiss LSM780 multiphoton confocal microscope fitted on an Axiovert M200 inverted microscope equipped with C-Apochromat (X40 = 1.2 numerical aperture) water immersion objectives (Carl Zeiss). Optical sections of minimum 1024X1024 pixels were collected sequentially for each fluorochrome. The data sets generated were merged and displayed with the ZEN software. Images from Images from figures 4 B, C, H, I were acquired with EC-Plan Neofluoar 10X/0.30 M27 objective. Image from Figure 2B was acquired on an Axio Observer Z1 Microscope using X40 Zeiss EC Plan-NEOFLUAR objectives, with an AxioCamMR3 camera and using the Axiovision software (Carl Zeiss).

Mammary cell preparation. MGs were dissected and the lymph nodes removed before processing. Samples were washed in HBSS and cut in pieces of 1 mm^3 with scissors. Samples were digested for 2h at 37°C under shaking in 300U/ML collagenase (Sigma)/ 300 µg/ml hyaluronidase (Sigma) in HBSS. EDTA at a final concentration of 5 mM was added for 10 min to the resultant organoid suspension, followed by 0.25% Trypsin/EGTA for 2 min. Samples were then filtrated through 40-µm mesh and rinsed in 2% FBS/PBS.

Cell labelling and flow cytometry. All steps of cell labelling were performed in PBS supplemented with 2% bovine serum. Two million cells per condition were incubated

in 500 µl primary antibody dilution for 30 min on ice, with shaking every 10 min. Primary antibodies were washed and cells incubated with secondary antibodies, with shaking every 10 min. Secondary antibodies were washed and cells were resuspended in 2.5 µg/ml DAPI (Invitrogen) before analysis.

Primary antibodies used were: APC-conjugated anti-CD45 (1/100, clone 30-F11, 17-0451, eBiosciences), APC-conjugated anti-CD31 (1/100, clone 390, 17-0311, eBiosciences), APC-conjugated anti-CD104a (1/100, clone APA5, 17-1401, eBiosciences), PECy7-conjugated anti-CD24 (1/100, clone M1/69, 560535, BD Biosciences), AlexaFluor700-conjugated anti-CD29 (1/100, clone HMβ1-1, 102218, Biolegend), PE-conjugated anti-CD49b (1/100, clone DX5, 553858, BD Biosciences), PerCP/Cy5.5-conjugated anti-Sca1 (1/100, clone D7, 108124, Biolegend), Biotin-conjugated anti-CD133 (1/100, clone 13A4, 13-1331, eBiosciences). Secondary antibody used was: APC-Cy7-conjugated streptavidin (1/400, 554063, BD Biosciences).

For BrdU staining, cells suspension from 4w and 10w old CD1 mice injected with 50mg/kg 5-Bromo-2-deoxyuridine (Sigma, B5002) 8h prior to analysis were stained as described above followed by BrdU staining using BD BrdU Flow kit (BD Biosciences 552598) using manufacturer's instruction except that anti-BrdU FITC (1/50, BD Biosciences 347583) was used instead of the one provided in the kit.

Data analysis was performed on a FACS Fortessa using the FACS DiVa software (BD Biosciences).

Mammary fat pad transplantation and analysis. One 1mm^3 non digested MG fragment coated with matrigel or 100000 unsorted mammary cells resuspended in 10 µl 75% DMEM/ 25% matrigel were injected into the number 4 glands of 4w old NodScid female mice that had been cleared of endogenous epithelium. Recipient mice

were mated 4 weeks after the transplantation, and were killed 10 days later, at mid-pregnancy. Recipient glands were dissected, fixed and embedded in OCT for analysis by immunofluorescence. An outgrowth was defined as an epithelial structure comprising ducts and branchings.

Quantification of ER+ LCs

For quantification of proportion of ER+ cells within LCs in figure 1B, 3 mice per time point were analyzed and a total of 213, 349, 364, 1497 and 515 LCs were analyzed respectively for P7, 5w, 8w, pregn and invo.

Quantification of YFP+ in ER+ LCs

For quantification of proportion of YFP+ cells within ER+ LCs described in figure 2N, 4 mice were analyzed per time point and a total of respectively 2335 and 2485 ER+K8+ cells were analyzed.

Quantification of YFP+ in CD24+CD29low LCs

For quantification of YFP+ cells in CD24+CD29low population described in figure 2G and 2S, respectively 3, 4, 3 and 4 mice were analyzed for no, 3d, 4w and 10w time points and minimum 100000 CD24+CD29low cells were analyzed per sample.

For quantification of YFP+ cells in CD24+CD29low population described in figure 3J, respectively 3, 4, 4 and 4 mice were analyzed for 4w, pregn, invo and 2nd invo time points and minimum 100000 CD24+CD29low cells were analyzed per sample.

Quantification of BrdU+ in LCs

Quantification of BrdU incorporation shown in figure 1C was performed in respectively 5 and 4 mice for 4w and 10w time points and a minimum of 10000 LCs were analyzed per sample.

Quantification of absolute number of LCs

For assessing the absolute number of LCs, total number of cells in samples was counted after cell preparation using Neubauer Improved cell counter (Blau Brand). FACS staining was performed as described above, and fraction of the different populations compared to total cells was analyzed based on FACS analysis. Absolute number of LCs was calculated by multiplying the total number of cells counted by the fraction of the LCs compared to total cells on FACS analysis.

For quantification of number of CD24+CD29low cells at 4w and 10w described in Figure 2H, 2 inguinal glands (one #4 and one #5 glands) from female CD1 mice were processed per sample. 10 mice were analyzed per time point.

For quantification of number of CD24+CD29low and YFP+ CD24+CD29low cells in adult and pregnant mice, 3 thoracic glands (one #1, one #2 and one #3) from female 10w old virgin or 2w pregnant ERrtTA/TetOCRE/Rosa-YFP mice were processed. Respectively 6 and 4 mice were processed in adult and pregnancy.
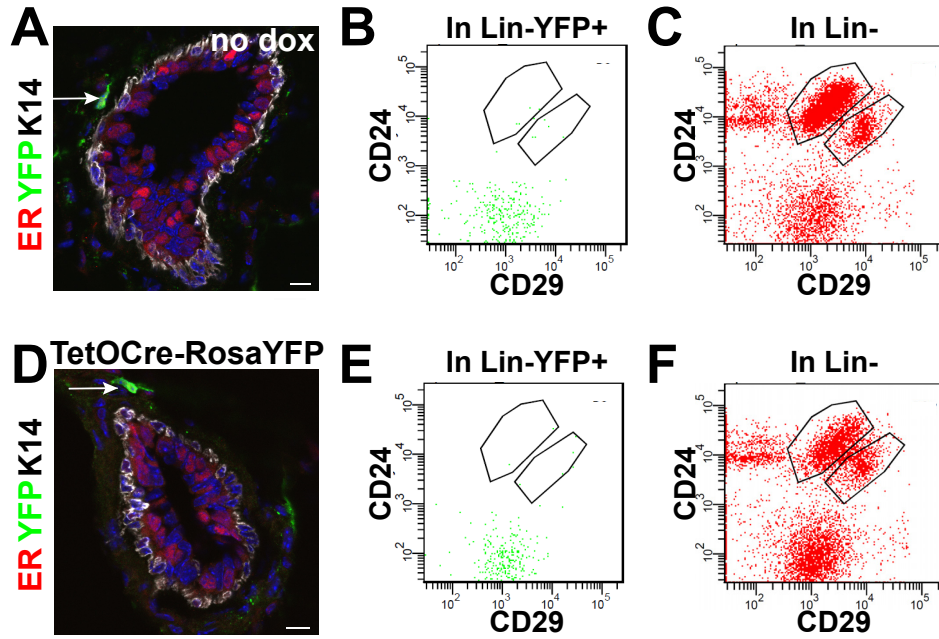
Supplemental Figure S1. Leakiness of TetOCre transgene in mesenchyme cells of the MG. Related to Figure 2. A-C, 5 weeks old ER-rtTA/TetOCre/RosaYFP mice without Dox treatment showing labelling of mesenchymal cells in the MG. A, Immunostaining of ER (red), YFP (green), K14 (white) and nuclei (blue). Arrow points to a YFP+ cell in the mesenchyme. **B,** C. FACS analysis of CD24 and CD29 in YFP+ cells **(**B) and in Lin- cells **(**C) show that YFP+ CD24- are observed without Dox treatment. **D**-F, 5 weeks old TetOCre/RosaYFP mice without Dox treatment also showing labelling of mesenchymal cells in the MG, demonstrating that the leakiness is due to TetOCre and not ER-rtTA transgene. D, Immunostaining of ER (red), YFP (green), K14 (white) and nuclei (blue). Arrow points to a YFP+ cell in the mesenchyme. **E,** F. FACS analysis of CD24 and CD29 in YFP+ cells **(**E) and in Lin- cells **(**F) show that YFP+ CD24- are observed in TetOCre/RosaYFP mice
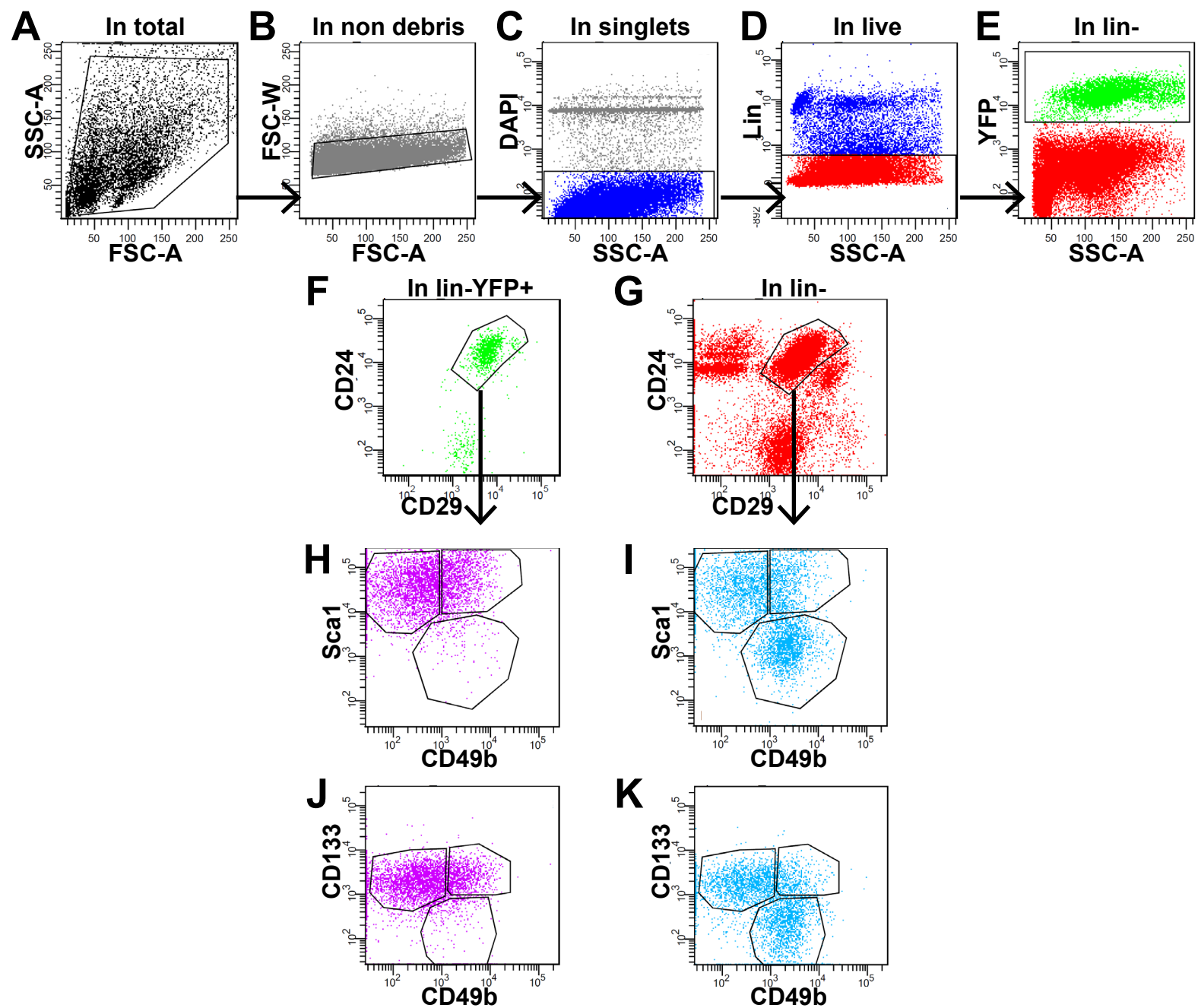
Supplemental Figure S2. FACS analysis of Sca1, CD133 and CD49b expression in LCs. Related to Figure 2. A-E, Unicellular suspension of mammary cells from ER-rtTA/TetOCre/RosaYFP mice (in this example, induced at puberty and analyzed 3d later) stained for Lin (CD31, CD45, CD140a), CD24, CD29, Sca1, CD133 and CD49b were gated as shown in **A** to eliminate debris, doublets were discarded with gate shown in **B**, the living cells were gated by DAPI dye exclusion as shown in **C**, the non-epithelial Lin positive cells were discarded in **D**, and the YFP+ cells were gated as shown in **E**. **F, G**, CD24 and CD29 expression was studied in YFP+ cells (**F**) or in Lin- cells (**G**) to define the CD24+CD29low luminal population. **H, I**, Sca1and CD49b expression was studied in luminal YFP+ cells (**H**) and in total luminal cells (**I**). **J, K**, CD133 and CD49b expression was studied in luminal YFP+ cells (**J**) and in total luminal cells (**K**).